Title: Island biogeography revisited: Museomics reveals affinities of shelf island birds determined by bathymetry and paleo-rivers, not by distance to mainland

Kritika M. Garg,[1,2,3]* Balaji Chattopadhyay,[1,4] Emilie Cros,[1] Suzanne Tomassi,[5] Suzan Benedick,[6] David P. Edwards,[5] Frank E. Rheindt[1]*

[1]Department of Biological Sciences, National University of Singapore, Singapore

[2]Centre for Interdisciplinary Archaeological Research, Ashoka University, Sonipat, India.

[3]Department of Biology, Ashoka University, Sonipat, India.

[4]Trivedi School of Bioscience, Ashoka University, Sonipat, India.

[5]Department of Animal and Plant Sciences, University of Sheffield, Sheffield, UK.

[6]Faculty of Sustainable Agriculture, University of Malaysia, Sabah, Malaysia.

*Corresponding authors: Kritika M. Garg (kritika.garg@ashoka.edu.in) and Frank E. Rheindt (dbsrfe@nus.edu.sg)

ABSTRACT

Island biogeography is one of the most powerful subdisciplines of ecology: its mathematical predictions that island size and distance to mainland determine diversity have withstood the test of time. A key question is whether these predictions follow at a population-genomic level. Using rigorous ancient-DNA protocols, we retrieved ~1000 genomic markers from ~100 historic specimens of two Southeast Asian songbird complexes from across the Sunda Shelf archipelago collected 1893–1957. We show that the genetic affinities of populations on small shelf islands defy the predictions of geographic distance and appear governed by Earth-historic factors including the position of terrestrial barriers (paleo-rivers) and length of persistence of corridors (Quaternary land bridges). Our analyses suggest that classic island-biogeographic predictors may not hold well for population-genomic dynamics on the thousands of shelf islands across the globe, which are exposed to dynamic changes in land distribution during Quaternary climate change.

INTRODUCTION

Islands contribute disproportionately towards our understanding of the evolutionary process (MacArthur and Wilson 1967; Whittaker et al. 2017). They provide a window into the workings of the evolutionary forces of isolation, migration, speciation and extinction, as well as the interactions among them (Borregaard et al. 2016; MacArthur and Wilson 1967; Whittaker et al. 2017). MacArthur and Wilson's (1967) seminal work on island biogeography suggested that the two main factors determining the species diversity of a given island depended upon its area and distance from the mainland. However, island size and distance to mainland may not provide a complete picture (Borregaard et al. 2016; Fernández-Palacios et al. 2016; Weigelt et al. 2016; Whittaker et al. 2017), with the role of Quaternary glaciations and concomitant sea-level fluctuations also pertinent to island biogeography (Fernández-Palacios et al. 2016; Weigelt et al. 2016). Cyclical periods of global cooling and warming over the past ~2.6 million years have not only been an engine of diversification at higher latitudes and altitudes, but also affected gene flow and speciation patterns in shelf-island regions (i.e. islands on continental shelves), especially in Southeast Asia (Brown et al. 2013; Chattopadhyay et al. 2017; Cros et al. 2020a; Garg et al. 2018; Garg et al. 2020; Heaney 1986; Hewitt 2000; Hewitt 2004; Lim and Sheldon 2011; Moyle et al. 2009; Ng et al. 2017; Rheindt et al. 2020). Many present-day shelf-islands have been connected by land bridges during cooler Quaternary periods with lower sea levels, allowing for possible dispersal of terrestrial organisms and gene flow (Cros et al. 2020a; Garg et al. 2018; Leonard et al. 2015; Lim et al. 2011; Lim et al. 2017; Lim and Sheldon 2011; Ng et al. 2017).

A key question is understanding the mechanisms by which Quaternary land bridges provide a conduit of gene flow for terrestrial organisms. Such land bridges can be highly species-specific conduits of gene flow, depending upon ecological requirements, and may be semipermeable by allowing more gene flow in one direction than in the other (Cros et al. 2020a; Garg et al. 2018). However, a precise quantification of the amount of gene flow that is facilitated by Quaternary land bridges remains problematic, as many organismic groups are capable of active or passive overwater dispersal (Mayr et al. 2001), obviating the need to evoke land bridges as the sole explanatory variable for dispersal events among present-day shelf-islands (Ng et al. 2017).

In this study, we directly tested the importance of Quaternary land bridges in facilitating gene flow through population-genomic analysis of two terrestrial rainforest songbird species

complexes across the Sundaic Region ('Sundaland') in Southeast Asia. Sundaland constitutes the most complex shelf-island archipelago in the world, encompassing the present-day landmasses of Sumatra, Java, Borneo, Peninsular Malaysia (henceforth: the Peninsula), plus numerous satellite islands (Fig. 1), and has undergone the most pronounced changes in land distribution globally across the Quaternary cooling cycles of the past 2.6 million years. During Quaternary cooling cycles, sea levels drop as water is locked up in the form of ice at higher latitudes, leading to the emergence of land bridges connecting Sumatra, Java, Borneo and numerous smaller islands with the mainland, forming Sundaland (Fig. 1). The widely disjunct historic distribution of orangutans and Asian rhinoceroses on disjunct islands, separated by ~500 km of open sea, bears testament to the frequent occurrence of connecting land bridges in the recent past (Mays et al. 2018; Nater et al. 2017). Consequently, Sundaland has become one of the main model regions to test impacts of Quaternary sea level change on evolutionary processes (Cros et al. 2020a; Leonard et al. 2015; Lim et al. 2011; Lim and Sheldon 2011; Lim et al. 2017)

We leveraged historic museum specimens collected during the 1800s and early 1900s to include samples from remote islands that are difficult to sample in modern times. By determining the genomic affinity of populations on key strategic island groups, we disentangle overwater dispersal from terrestrial dispersal across past land bridges. The study of underwater depth—bathymetry—is important in determining the level of island isolation: for instance, while the small Natuna islands are geographically close to Borneo, bathymetric data indicate that their land connection to Borneo severed far earlier than did their connection to Sumatra and the Peninsula (Fig. 1). A genomic affinity of Natuna populations with those on Sumatra or the Peninsula, despite Natuna's proximity to Borneo, would be a powerful indication that gene flow among these birds is purely governed by the distribution of Quaternary land bridges. Equally, a closer affinity with Borneo would argue for considerable levels of overwater dispersal, especially during periods when intervening water distances were smaller.

We focus on two widespread and characteristic Sundaic bird species complexes, the black-capped babbler (*Pellorneum capistratum*) and short-tailed babbler (*P. malaccense*), both sedentary rainforest denizens foraging in the understory (Eaton et al. 2016). Both these songbirds are known for their ubiquitous occurrence across a wide range of Sundaic lowland and hill rainforests and their general inability to cross even narrow non-forest gaps, especially

open water (e.g. Cros et al. 2020b; Sadanandan and Rheindt 2015; Zakaria et al. 2013). We characterized and compared variation in plumage patterns using a series of museum specimens to assess whether morphological differentiation is congruent with the population-genomic signal. Museums are a treasure trove of important phenotypic and genomic information from remote areas. However, DNA from century-old museum specimens, especially from the tropics, is often heavily degraded and only minuscule amounts can be salvaged (Chattopadhyay et al. 2019; Dabney et al. 2003). Hence, we used a target capture approach to ensure high quality genome-wide data would be obtained from multiple samples. This approach has been successfully utilized previously for similarly degraded samples (Chattopadhyay et al. 2019). At the same time, we implemented multiple cleanup steps and analytical approaches to account for excess DNA damage and increased levels of C to T and G to A substitutions in the ancient DNA of our samples (Chattopadhyay et al. 2019; Dabney et al. 2003).

We harvested ~1000 genome-wide sequence loci targeting ~1% of the genomes and employed modern approaches of admixture analysis, allowing us to shed light on patterns of isolation and divergence across Sundaland and the role of Quaternary land bridges in dictating dispersal. We tested whether distance to the mainland is the main determinant of population genomic patterns, or whether bathymetric data—reflective of Quaternary land bridges and the course of paleo-rivers—define the population genomic structure of our target species. Based on the first hypothesis, the population genomic affinity of small-island bird populations, e.g. on Natuna, will be similar to that of birds from nearby Borneo (Fig. 1). However, if the history of land connections is more important, then the affinity of these island populations should be with populations from the Peninsula and Sumatra (Fig. 1).

RESULTS

Plumage analysis

We compared the plumages of museum specimens of *P. capistratum* and *P. malaccense* (see Supplementary Table 1) deposited at the Lee Kong Chian Natural History Museum (Singapore). Within the *P. capistratum* complex, we observed three groups based on plumage. The most striking plumage difference among populations was the color of the supercilium, which divided specimens into (1) a cluster in western Sundaland (subspecies *P. c. nigrocapitatum*; Peninsula, Sumatra and Natuna) characterized by a grey supercilium with

thin white shaft streaks, (2) a Bornean cluster (subspecies *P. c. capistratoides* at least from Sarawak and *P. c. morrelli* at least from Sabah) with a wholly white supercilium, and (3) a Javan cluster (subspecies *P. c. capistratum*) with an orange anterior and white posterior supercilium (Supplementary Figs. 1A, 1B and 1C). Similarly, lores were white or pale grey in Javan specimens, mid-grey in western Sundaic specimens, and dark grey in Bornean specimens (Supplementary Figs. 1A, 1B and 1D). All western Sundaic specimens had a black moustachial stripe (Supplementary Fig. 1C) that was absent in Javan and Bornean specimens. Additionally, specimens from Java had a paler tail and back than all other populations (Supplementary Fig. 1D), and a uniquely orange lateral suffusion on the white throat.

In western Sundaland, we observed consistent differences across specimens from the Thai-Malay Peninsula, Sumatra, and Natuna. Specimens from the Peninsula had a brownish black crown while Natuna and Sumatran specimens usually had a more saturated black crown. Similarly, on Borneo, specimens from Sabah had a paler orange belly and breast than specimens from Sarawak. Interestingly, Sarawak specimens' belly and breast coloration resembled that of specimens from western Sundaland. We did not compare the coloration of legs, bills and iris due to post-mortem color change and incomplete label data.

We observed a high variability in plumage within the *P. malaccense* complex, much of it seemingly independent of location (Supplementary Figs. 1E, 1F and 1G). Nevertheless, a few geographically consistent differences did emerge: Bornean populations (subspecies *P. m. poliogene* and *P. m. saturatum*) differed from those in western Sundaland (subspecies *P. m. malaccense*) in having a more olive rather than chestnut back (mantle and wings) (Supplementary Figs. 1E, 1F and 1G). Within Borneo, specimens from Sabah (subspecies *P. m. poliogene*) exhibited a more rufous tail while specimens from Sarawak showed a less warm-colored brown tail (Supplementary Figs. 1E and 1G). Interestingly, all the other differences between Sarawak and Sabah also differentiated Sarawak populations from western Sundaland. Specimens from Sarawak appeared the most distinct population based on plumage alone: they had a darker crown, darker ear coverts and darker moustachial stripe than all other taxa. They also had more intensely orange flanks and breast whereas other populations had paler, more apricot-colored flanks and breast (Supplementary Fig. 1E). Again, comparisons of the coloration of legs, bills and iris were impossible because of post-mortem color change and a lack of sufficient label information.

205 **Sampling, DNA extraction and raw data filtering**

206 We obtained toepads of specimens of both *P. capistratum* (n = 50) and *P. malaccense* (n =
207 46) from the Lee Kong Chian Natural History Museum (Singapore) and Yale Peabody
208 Museum of Natural History (New Haven, Connecticut) (Supplementary Table 1). These
209 specimens were collected over a period of ~70 years from 1893 to 1957. All historical
210 samples were processed in a separate dedicated facility and with fresh gloves, forceps and
211 scalpels for each sample to avoid cross contamination.
212
213 We successfully isolated DNA from ~80% of historic samples (n = 77). Presence of DNA
214 was confirmed using Qubit and an AATI Fragment Analyzer. No detectable DNA was
215 observed in negative controls. All 77 samples along with negative controls were further
216 processed for library preparation and target enrichment. Target enrichment protocols have
217 been shown to be highly effective for ancient DNA samples (Chattopadhyay et al. 2019). We
218 designed target loci (960 loci) for sequence capture protocols that are useful for both
219 population genomic and phylogenomic studies targeting both conserved exons and variable
220 intronic regions (see methods for details). We supplemented historical DNA with fresh
221 samples from Sabah (n = 12) (Supplementary Table 1) following the fieldwork protocols of
222 Cros et al. (2020a). All enriched libraries were sequenced on multiple lanes of HiSeq 4000
223 (150bp paired end runs). The fresh samples from Sabah were processed separately and
224 sequenced in a dedicated lane. We retained ~0.97 billion reads after cleanup steps
225 (Supplementary Table 1). The average number of reads per sample was ~11 million (standard
226 deviation = ~5 million).
227
228 **Data matrix**

229 For DNA sequence-based analysis, we obtained sequence data for 944 out of 960 target loci
230 designed for both species complexes using the HybPiper pipeline. We removed ten historic *P.*
231 *malaccense* samples from downstream processing as their missing data exceeded 85%. After
232 multiple sequence alignments, we performed stringent filtering of alignments using Gblocks
233 and removed 117 loci from the *P. capistratum* dataset and 385 loci from the *P. malaccense*
234 dataset due to high missing data. After removal of loci < 200bp and Z-chromosomal loci, we
235 retained 652 loci for *P. capistratum* and 314 loci for *P. malaccense*. The total sequence
236 matrix length for *P. capistratum* was 454,712 bp (average locus length = 697 bp; minimum =
237 201 bp; maximum = 4,723bp) and 145,877 bp for *P. malaccense* (average locus length = 465
238 bp; minimum = 201 bp; maximum = 2,607 bp).

For SNP-based analysis, we generated four different datasets for each species complex (dataset I: all SNPs obtained after mapping to *Mixornis gularis* genome; dataset II: only transversions obtained after mapping to *Mixornis gularis* genome; dataset III: single random SNP per target locus; dataset IV: only transversions obtained after mapping to *Parus major* genome). We retrieved between 960 and 208,186 SNPs for *Pellorneum capistratum* and between 958 and 198,711 SNPs for *P. malaccense* across datasets before filtering (Table 1). For dataset IV, after filtering for linkage, deviations from Hardy-Weinberg equilibrium, neutrality and DNA damage, we retained 40,611 transversions for *P. capistratum* and 34,809 transversions for *P. malaccense*. As admixture graph analysis can accommodate SNPs located on the Z chromosome, we included these in our analysis of gene flow. In contrast, for analyzing population structure, we removed the outgroup and any resulting monomorphic loci along with SNPs located on the Z chromosome and retained 38,463 transversions for *P. capistratum* and 32,735 transversions for *P. malaccense* (Table 1). The overall level of missing data for dataset IV was less than 10% for both species after all cleanup steps. For the other datasets the number of SNPs after cleanup is summarized in Table 1.

Phylogenomic reconstruction

We used both concatenation approaches and species tree reconstruction for phylogenomic analysis (see Methods). Sumatran and Natuna populations were embedded within the peninsular population based on the concatenated maximum likelihood trees in both species complexes (Supplementary Figs. 2A and 2C). Our sole *P. malaccense* individual from the Anambas archipelago (Fig. 1) also formed part of the large peninsular clade (Supplementary Fig. 2C). In *P. capistratum*, the Javan population was distinct from both peninsular/Sumatran and Bornean populations, emerging as sister to the latter (Supplementary Figs. 2A and 2B). In the case of *P. malaccense*, the Sabah population formed a clade distinct from Sarawak and basal to all members of the complex (Supplementary Figs. 2C and 2D).

Population structure

We employed multiple approaches to understand population structure within each babbler species complex and observed similar trends of subdivision across all four SNP datasets generated in this study (Figs. 2 and 3, Supplementary Figs. 3–8). Principal component analysis (PCA) and discriminant analysis of principal components (DAPC) suggested three distinct population groupings in each complex in agreement with phylogenomic results (Figs.

2A, 2B, 3A and 3B, Supplementary Fig. 2). In *P. capistratum*, the division entailed (1) a western Sundaic group comprising populations from the Peninsula, Sumatra and Natuna, (2) a Javan group, and (3) a Bornean group (Fig. 2, Supplementary Figs. 3–5). In *P. malaccense*, Bornean populations separated into two deeply divergent groups, one from Sarawak and the other from Sabah (Fig. 3, Supplementary Figs. 6–8) in agreement with previously published studies based on mitochondrial DNA (Lim and Sheldon 2011; Sadanandan and Rheindt 2015) and the phylogenomic analysis presented in this study (Supplementary Figs. 2C, and 2D). The Sarawak cluster emerged as more closely related to the third group consisting of individuals from the Peninsula, Sumatra, Natuna and Anambas (Fig. 3, Supplementary Figs. 6–8).

The results based on the Bayesian clustering program STRUCTURE were congruent with other analyses for *P. capistratum*, in which the western Sundaic cluster (Peninsula, Sumatra, Natuna) separated from the other clusters (Borneo and Java) at K=2 (Fig. 2C), with the latter two separating at K= 3 (Fig. 2C, Supplementary Figs. 3C, 4C, 5C). STRUCTURE results were less clean for *P. malaccense*, in which only Sabah emerged as clearly distinct for K=3 (and sometimes K=2), whereas the Sarawak cluster did not emerge as visually distinct before K=4 (Fig. 3C, Supplementary Figs. 6C, 7C and 8C).

Gene flow dynamics

The application of D-statistics and admixture graph analysis allowed us to infer the complicated nature of gene flow events and dynamics among populations of all the major Sundaic landmasses investigated (Figs. 4 and 5; Supplementary Table 2). For *P. capistratum*, 781 out of 63,725 possible graphs tested by qpbrute exhibited a fit with our data when considering all populations. As this number of graphs was computationally intractable for Bayes factor estimation, we performed subsequent qpbrute analysis in two steps. Initially, we included all populations other than Natuna in our analysis and obtained 41 possible solutions. After Bayes factor estimation, we selected ten graphs as the most likely starting models. For the selected ten graphs, we then included the Natuna population, resulting in 12 unique graphs. Following another round of Bayes factor estimation, five of these admixture graphs displayed a good fit with the data (Fig. 4A). These five admixture graphs had identical topologies and only differed slightly in estimates of admixture proportions for the western Sundaic populations (Fig. 4). They suggested a lack of substantial gene flow between

lineages from Java, Borneo and western Sundaland, but pronounced allelic contributions into the three western Sundaic populations from unsampled sources, likely now-extinct populations from the north.

We obtained a single possible admixture graph for *P. malaccense* out of 9,083 unique graphs tested by qpbrute (Fig. 5). This graph supported post-divergence gene flow from Sabah into western Sundaic populations but not into the adjacent Sarawak population, indicating a potentially strong reproductive barrier between the two Bornean lineages. It also suggested various streams of ancestral allelic contributions into most western Sundaic populations from unsampled, possibly extinct sources (Fig. 5).

DISCUSSION

Bathymetric topography predicts genomic affinity of island populations

For both songbird species complexes under study, all phylogenomic and population-genomic approaches unanimously confirmed that Natuna and Anambas island populations are firmly embedded with the peninsular—not Bornean—population cluster (Fig. 2 and 3; Supplementary Figs. 2–8). These conclusions were further corroborated by plumage analysis (Supplementary Fig. 1). These insights defy the fact that Natuna is only ~220 km from the nearest populations on Borneo, less than half (~46%) the distance to the nearest population in Peninsular Malaysia (~480 km) (Fig. 1). Our results unequivocally support the hypothesis that the history of land connections, as dictated by sea level changes and bathymetry, has determined the genetic affinity of shelf-island populations, and that overwater dispersal-related processes have been of much less importance.

The distance of an island to the nearest mainland has long served as one of the central tenets of classical island biogeography in making inferences about island biota (MacArthur and Wilson 1967). Geographic distance to the mainland has been accepted as the natural criterion explaining why many island biotas are exclusively recruited from one landmass versus the other. Well-documented examples include the American origin of most species inhabiting Bermuda (Sterrer et al. 2004), the European provenance of most species on the Azores (Wallace 1872), and the affinities of British animal populations with those from nearby France, rather than with Scandinavian or Central European populations that share more

similarities in climatic regimes they are adapted to (Hewitt 2000; Hewitt 2004; Taberlet et al. 1998; Teacher et al. 2009).

An improvement in our understanding of paleo-climate has led to a realization of the importance of Quaternary sea level change in defining the evolutionary history of terrestrial biota (Cros et al. 2020a; Garg et al. 2018; Lim et al. 2011; Heaney et al. 2005; Ng et al. 2017), and has resulted in a new appreciation of bathymetry as a crucial indicator of the extent of land bridges which existed only a few thousand years ago (Garg et al. 2018; Rheindt et al. 2020). Inspection of the bathymetric profile of Sundaland suggests that the land connection between the Peninsula and Natuna/Anambas persisted ~1000 years longer than between Borneo and Natuna/Anambas (Sathiamurthy and Voris 2006) (Fig. 1), supporting the importance of bathymetry and paleo-island distribution in determining the genomic composition of smaller island populations. At the macro-evolutionary level, a re-analysis of species diversity patterns across the planet has shown that Quaternary land connections are an important but overlooked parameter in defining island species diversity (Weigelt et al. 2016) and faunal turnover (Lohman et al. 2011). For instance, one of the steepest and most renowned faunal transition zones runs across Wallace's line (Lohman et al. 2011; Huxley 1868; Wallace 1860), separating Sundaland from the Australo-Papuan faunal region. Although only separated by narrow straits, land masses to the east and west of Wallace's line harbor biota of extremely different affinities, attesting to the importance of the deep sea trenches that have precluded the formation of land bridges across this narrow gap (Wallace 1860).

At the population-genetic level, there has so far been a distinct lack of understanding whether the genomic composition of terrestrial populations on present-day shelf islands is largely defined by geographic distance to the nearest large landmass, or by bathymetric topography and consequently by the duration of land connections during the Pleistocene. Genome-wide markers have been instrumental in answering whether shelf island populations are mostly the product of overwater dispersal or of dispersal across historic land connections, which would be difficult to ascertain based on phenotypic data alone (Ng et al. 2017). As Quaternary glacial cycles leave a track record within the genome, patterns of genomic diversity can be used to reconstruct evolutionary history (Cros et al. 2020a; Garg et al. 2018; Lim et al. 2017; Ng et al. 2017; Papadopoulou and Knowles 2017; Rheindt et al. 2020).

Paleo-rivers: a long-overlooked determinant of population-genetic structure

The role of big rivers in shaping population structure in large areas of tropical rainforest has received much interest. In South America, the Amazon River and its tributaries are known as important barriers between neighboring subspecies and closely related species, many of which have recently been taxonomically upgraded with an improved biological understanding (Burney and Brumfield 2009; Islet et al. 2001; Isler and Maldonado-Coelho 2017; Rheindt et al. 2008; Rheindt et al. 2009). Likewise, in Africa, the Congo River is an important divide between young, recently separated species (Prüfer et al. 2012). In Southeast Asia, on the other hand, most rainforest is fragmented archipelagically, and open sea dividing different islands is considered the main shaping force of population structure, with rivers afforded a minor role (Cros et al. 2020a; Lim et al. 2011; Lim et al. 2017; Lohman et al. 2011; Mason et al. 2019). At the same time, the present division of Sundaland into a handful of large and numerous smaller islands only represents a snapshot in time, as all larger landmasses in Sundaland have been connected by land bridges for a cumulative ~90% of the last one million years (Cannon et al. 2009; Mason et al. 2019; Sarr et al. 2019). Therefore, rivers may have played a much larger role in shaping population structure here than previously appreciated.

Our historic museum samples did not encompass a sufficient number of sites to systematically test the divergence effects of large paleo-rivers in Sundaland. However, it did allow us to inspect whether population-genetic divisions are consistent with the river barrier effect specifically in the case of the two small shelf-island archipelagos of Natuna and Anambas. During the global sea-level lows, Natuna has been connected to the Peninsula further west by a hilly watershed with adjacent flat valleys, covered by evergreen tropical rainforest ideal for the babblers under study (Bird et al. 2005; Cannon et al. 2009). On the eastern side, a large paleo-river, the North Sunda River, originating in the Central Sumatran mountains and debouching in the South China Sea, separated Natuna from Bornean land extensions further south (Bird et al. 2005; Voris 2000) (Figs. 4 and 5). Natuna is situated close to the former delta of the North Sunda River, which is the longest exclusively Sundaic river during times of land emergence (Voris 2000). With its length of almost 2,000km forming a vast tropical rainforest watershed, it would have featured a wide lower course and delta, and would have been equivalent in impact to some Amazonian tributaries of similar length, e.g. the Xingu River, that are also known to constitute important population-genetic barriers (da Costa et al. 2016; Isler and Maldonado-Coelho 2017). Paleo-rivers, which have

hitherto been afforded little importance in accounting for population subdivisions in Sundaland, offer a compelling explanation for Natuna's deeper genetic rift from Borneo: Natuna's placement just north-west of the delta of the North Sunda Paleo-River, the largest tropical Asian river at the time, would have prevented small and poorly dispersive forest inhabitants from easily crossing over towards Borneo even at times when extensive land connections existed.

Our data indicate that Sundaic paleo-rivers other than the North Sunda River may also have had an important imprint on population structure. North of present-day Natuna and Anambas, the Siam Paleo-River system constituted an extension of the present-day Chao Phraya, the most dominant river in the Thai plains (Figs. 4 and 5), extending the length of the latter 2–3 fold during periods of land emergence (Voris 2000). North of the Siam river, there would have been extensive areas of lowland rainforest that are largely submerged now (Cannon et al. 2009), but have historically survived at the southernmost tip of Vietnam, where a number of Sundaic vertebrates have their northernmost isolated outposts (for examples see Robson 2005). *P. malaccense* and *P. capistratum* no longer occur in this Sundaic outpost but may have survived in this area into the present interglacial and gone extinct as a result of the historic destruction of all rainforests here. An ancestral allelic contribution of 10% in the Anambas population of *P. malaccense* from an unsampled, possibly extinct population may well relate to gene flow across the Siam Paleo-River from a diverged northern population that still existed there at the time (Figs. 4 and 5). By the same token, a similar ancestral allelic contribution of 9-16% into the Natuna population of *P. capistratum* may reflect gene flow from a northern, now-extinct stronghold across the Siam Paleo-River into populations that are now stranded on Natuna.

Importance of museum collections

Our study demonstrates the timeless importance of historic specimen collections for evolutionary research. In modern times when DNA collection is becoming ever more restrictive, one of the best paths to comprehensive genomic sampling is through historic museum collections. Ancient DNA is prone to degradation and damage through an excess in C to T and G to A substitutions, and the implementation of multiple safeguards is necessary to avoid bias in DNA sequence generation from historic specimens. Our study highlights the utility of target enrichment methods to isolate homologous genomic regions across multiple degraded historic museum samples, and to harvest the DNA signal of hundreds of genomic

markers which can capture both phylogenomic and population genomic information. Our study was based on specimens containing highly degraded DNA from the Lee Kong Chian Museum (formerly the Raffles Museum) in Singapore, held at tropical temperatures for many decades before air-conditioning was introduced in the ~1980s. Our successful retrieval of thousands of genome-wide SNPs through the rigorous application of ancient DNA protocols to reduce artifacts due to excess damage demonstrates that even degraded historic museum material can serve an important purpose in molecular research. We hope this approach will be applied to numerous additional organismic groups across the tropics to solve evolutionary problems.

METHODS

Plumage analysis

We examined the plumages of 41 museum specimens of *P. capistratum* and 45 museum specimens of *P. malaccense* (Supplementary Table 1) deposited at the Lee Kong Chian Natural History Museum (Singapore). Specifically, we laid out specimen series arranged by geographic area and compared plumage hues for wings, tail, upperparts, underparts and head. We checked label information for the color of beak, legs and iris on live birds.

DNA extraction

DNA extractions of historical samples were performed in a separate dedicated ancient DNA facility within a biosafety cabinet. We used DNeasy Blood and Tissue Kits (QIAGEN, Germany) with modifications to extract highly degraded DNA (see Chattopadhyay et al. (2019) for details). We used one or two toepads per sample for DNA extraction. Prior to DNA extraction the toepads were washed two to three times with molecular grade water to remove any PCR inhibitors. We used 360µl of ATL buffer and approximately 100µl of Proteinase K per sample to digest the tissue. The toepads generally required approximately three to five days to completely digest. The volumes of AL buffer and ethanol were adjusted according to the total volume of ATL buffer and Proteinase K. We used Minelute columns (QIAGEN, Germany) for DNA extraction instead of the regular columns provided by the manufacturer as these can help elute single stranded DNA as well as small DNA fragments. As historical samples are highly degraded, these columns were helpful in isolating poor quality DNA. DNA extracted from historical samples was then quantified using an AATI

Fragment Analyzer as well as high sensitivity Qubit Assay kits (Invitrogen, USA). For all DNA extractions we carried through a negative control to detect possible contamination. For fresh samples, we extracted DNA from blood using DNeasy Blood and Tissue Kits following the manufacturer's instructions and quantified DNA using high sensitivity Qubit Assay kits.

Library preparation

We prepared whole genome libraries using NEB II Ultrakits (New England BioLabs, USA). For ancient samples we included an additional step of DNA repair using the FFPE DNA repair kit (New England BioLabs, USA) prior to library preparation. Historical samples are prone to DNA damage and this step reduced the levels of damage observed in later steps (Chattopadhyay et al. 2019). We carried through a dedicated negative control for each batch of library preparation. For fresh samples we used a bioruptor pico (Diagenode, Belgium) to fragment the DNA, performing 13 cycles of 30s ON and 30s OFF to obtain DNA fragments of ~250 bp. Samples were then subjected to library preparation using the NEB Ultra II kit. All samples were dual indexed using 8bp barcodes.

Design of target loci

Target enrichment protocols have been shown to be highly effective for ancient DNA samples (Chattopadhyay et al. 2019). We designed target loci for sequence capture protocols that are useful for both population genomic and phylogenomic studies targeting both conserved exons and variable intronic regions. We used EvolMarkers (Lim et al. 2012) to identify conserved single copy coding sequences in the striped tit-babbler genome (*Mixornis gularis*, QVAJ00000000.1), collared flycatcher genome (*Ficedula albicollis*, GCA_000247815.1) and zebra finch genome (*Taeniopygia guttata*, GCF_003957565.1). The striped tit-babbler genome is the phylogenetically closest genome available for both target species. To identify conserved exons, EvolMarkers performs a BLAST search, for which we set a minimum of 55% identity and e-value of less than 10E-15. Only exons longer than 500bp were used for downstream analysis. We identified a total of 1,161 exons. Then we isolated 500 bp upstream and downstream of these conserved exons from the striped tit-babbler genome to recover variable intronic regions using bedtools 2.28.0 (Quinlan and Hall 2010). We further checked for overlapping targets and merged all overlapping loci in bedtools. We then removed any loci with a GC content less than 40% or more than 60%. Loci which contained repeat elements were identified using RepeatMasker 4.0.7 (Smit et al. 2015) and removed. We finally retained 960 loci (1.99Mb), which were used by MYcroarry (USA)

to design RNA baits. We used 73,928 100bp baits with 4X tiling density for in-solution target enrichment.

Target enrichment

We performed in-solution hybrid capture for whole genome libraries to enrich target loci. A modified version of the myBaits (USA) protocol was used for hybridization (myBaits manual version 3). For ancient samples, we diluted the baits and used them at 50% strength, carrying out independent hybridization reactions at 60 ^{0}C for 40 hours. For fresh samples, we pooled three uniquely barcoded samples at equimolar concentrations and carried out hybridization at 65 ^{0}C for 20 hours. We used a lower temperature and longer duration for the hybridization of ancient samples as suggested by the MYBaits manual. Following hybridization, the samples were cleaned as suggested in the MYBaits manual and we performed PCR for the enriched libraries using IS5 and IS6 primers (Kircher et al. 2012). The final libraries were cleaned using Ampure beads and pooled at equimolar concentrations. We sequenced the enriched libraries on multiple lanes of HiSeq 4000 (150bp paired end runs). Fresh and ancient samples were run on separate lanes. All negative controls were also sequenced to rule out contamination.

Data filtering and cleanup

We obtained 1.4 billion 150bp paired-end reads. Reads with a PHREAD score below 10 were removed by the service provider. We ran FASTQC 0.11.7 (Andrews 2010) to check for adapter contamination. We used cutadapter 1.12 (Martin 2011) to trim adapters from the reads and performed another quality check in FastQC. Subsequently, we used Trimmomatic 0.38 (Bolger et al. 2014) to remove any remaining adapter sequences. Trimmomatic also removes any low-quality reads and reads less than 36bp in length. Finally, we performed a third FastQC run to check for sequence quality and confirm complete adapter removal. Next, we removed PCR duplicates using the dedupe program within bbmap 36.84 (Bushnell 2014). Furthermore, for the ancient samples we used mapDamage 2.0 (Jónsson et al. 2013) to remove preservation-related post-mortem substitutions. We observed high rates of transitions (G to A and C to T) at the ends of reads. Hence, we first rescaled our bam files using mapDamage. Then the rescaled bam files were converted to fastq reads and we trimmed 10bp from both the 5' and 3' ends in the historic samples using Seqtk 1.2-r94 (https://github.com/lh3/seqtk) to reduce bias due to DNA degradation. The cleaned reads were used for downstream processing.

543

544 **Data matrix generation**

545 We used two different approaches to generate data matrices for each of the two babbler
546 species complexes. In the first approach, we generated sequence data matrices for target loci.
547 In the second approach, we generated genome-wide SNPs.

548

549 **A. Sequence data generation**

550 To generate a sequence data matrix of target loci, we used the HybPiper 1.2 pipeline
551 (Johnson et al. 2016), which is specifically designed for sequence capture protocols. We
552 generated sequence data with an outgroup individual for phylogenomic analysis. The
553 resultant sequences were then aligned using MAFFT v7.130b (Katoh and Standley 2016). We
554 used auto settings within MAFFT to identify the best approach for sequence alignment. The
555 alignments were further cleaned using strict settings (default settings) within Gblocks 0.91b
556 (Castresana 2000) to remove poorly aligned regions. We further removed loci with a
557 sequence length less than 200bp and those located on the Z chromosome for phylogenomic
558 analysis.

559

560 We obtained sequence data for 944 out of 960 target loci designed for both species
561 complexes using the HybPiper pipeline. We removed ten historic *P. malaccense* samples
562 from downstream processing as their missing data exceeded 85%. After multiple sequence
563 alignments, we performed stringent filtering of alignments using Gblocks and removed 117
564 loci from the *P. capistratum* dataset and 385 loci from the *P. malaccense* dataset due to high
565 missing data. After removal of loci < 200bp and Z-chromosomal loci, we retained 652 loci
566 for *P. capistratum* and 314 loci for *P. malaccense*. The total sequence matrix length for *P.*
567 *capistratum* was 454,712 bp (average locus length = 697 bp; minimum = 201 bp; maximum =
568 4,723bp) and 145,877 bp for *P. malaccense* (average locus length = 465 bp; minimum = 201
569 bp; maximum = 2,607 bp).

570

571 **B. SNP data generation**

572 We generated four different SNP sets for each of the two babbler species complexes. For the
573 first three SNP sets, we mapped the clean reads to the striped tit-babbler genome using
574 BWA-MEM 0.7.17-r1188 (Li and Durbin 2009). The mapped reads were sorted and
575 converted to a bam format using SAMTOOLS 1.9 (Li et al. 2009; Li 2011). We used the
576 GATK SNP caller within ANGSD 0.923-3-ga8ed56f (Korneliussen et al. 2014) to identify

577 SNPs for each species complex separately. For both species complexes, we used a p-value
578 cut-off of 1E-6. Further, only SNPs with a PHREAD score ≥30 (99.9% accuracy) were
579 retained. We allowed for no missing data during SNP calling. The SNPs were further filtered
580 using VCFtools 0.1.16 (Danecek et al. 2011), and any locus with a read depth <10 per sample
581 was removed. We then removed linked loci using PLINK 1.9 (Purcell et al. 2007) by
582 applying the indep-pairwise algorithm with a sliding window size of 50 SNPs, a step size of
583 10 and an r^2 correlation coefficient cut-off of 0.9. We also removed any loci not in Hardy-
584 Weinberg equilibrium using PLINK while correcting the p-value for multiple comparisons.
585 We further tested for selection in BAYESCAN 2.1 (Foll and Gaggiotti 2008) using default
586 settings and removed any locus under positive selection. The striped tit-babbler genome was
587 also blasted to the chromosomal assembly of the great tit genome (*Parus major*,
588 GCA_001522545.3) using blastn to identify scaffolds which map to the Z chromosome. The
589 great tit genome is the phylogenetically closest genome available that has been assembled to
590 the chromosome level. SNPs which mapped to the Z chromosome of the great tit genome
591 were removed from downstream processing. The cleaned, unlinked, neutral autosomal SNPs
592 constituted dataset I. C to T and G to A substitutions are the most common post-mortem
593 substitutions observed in historic samples and hence can bias results (Chattopadhyay et al.
594 2019). To account for DNA damage due to historic sampling, we therefore generated a
595 second dataset in which only transversions were included in analyses (dataset II). We also
596 generated a third dataset which included only a single random SNP from each target locus.
597 We did not perform any test for linkage for this dataset (dataset III).
598
599 For the final dataset (dataset IV) we mapped clean reads to the great tit genome and carried
600 out SNP calling in ANGSD as mentioned above. We included an outgroup for this SNP set
601 and allowed for 20% missing data. We further pruned the dataset for linkage disequilibrium
602 and deviations from neutrality and Hardy-Weinberg equilibrium using the same approaches
603 as mentioned above. We only retained transversions for dataset IV. This latter dataset had the
604 advantage of chromosomal information required for admixture graph analyses (see section on
605 ABBA-BABA). For the population structure analysis using dataset IV, we further pruned the
606 loci located on the Z chromosome.
607
608 In the end, we retrieved between 960 and 208,186 SNPs for *P. capistratum* and retained 883
609 to 54,906 SNPs after filtering (Table 1). For *P. malaccense* between 958 and 198,711 SNPs

610 were obtained across datasets before filtering and we retained 895 to 33,708 SNPs for further
611 analysis (Table 1).
612
613 **Phylogenomic analysis**
614 We used both concatenation approaches and species tree reconstruction for phylogenomic
615 analysis. For concatenation-based analyses, we used RAxML 8.2 (Stamatakis 2014) to
616 reconstruct a maximum likelihood tree using the GTR+GAMMA model of substitution. We
617 ran the AMAS pipeline (Borowiec 2016) to concatenate loci. For species tree reconstruction,
618 we used the phyluce pipeline 1.6.6 (Faircloth 2016) to process the sequence data. We
619 generated individual maximum likelihood gene trees using RAxML within the phyluce
620 pipeline for downstream use in MP-EST 1.6 (Liu and Edwards 2010) to estimate the species
621 tree. We followed Liu et al. (2017) for species tree estimation and generated 100 bootstrap
622 trees per locus. We further generated 100 bootstrap files containing one bootstrap replicate
623 per locus. These files were then used for MP-EST species tree estimation. The 100 bootstrap
624 species trees were further used to estimate nodal support and to generate a majority-rule
625 consensus tree using Phylip v3.69 (Felsenstein 2005). Both the concatenated tree and species
626 tree were viewed in FigTree v1.4.2 (http://tree.bio.ed.ac.uk/software/figtree/).
627
628 **Population genomic analysis**
629 We employed multiple approaches to understand population subdivision within each babbler
630 species complex. First, we performed PCA using the SNPrelate package in R (Zheng et al.
631 2012). PCA is a multi-variate approach to identify structure within datasets, but is at the same
632 time independent of population genetic assumptions. For dataset IV we removed the loci with
633 missing data for PCA analysis. Second, we performed DAPC in the adegenet 2.1.1 R package
634 (Jombart 2008). One major feature that sets DAPC apart from PCA is that it tends to
635 maximize between-group differences while placing less emphasis on within-group
636 variability[73]. Finally, we adopted a Bayesian clustering approach using STRUCTURE
637 (Pritchard 2000) to identify subdivision within each species complex. We used the structure
638 threader program for STRUCTURE analysis and performed ten runs each for K=1 to 10. For
639 each K, we performed 100,000 burn-ins and 500,000 Markov chain Monte Carlo steps.
640 Structure runs were performed without any *a priori* assumptions of population assignment.
641 We ran the pophelper R package (Francis 2017) to visualize STRUCTURE results and
642 compared across multiple K values to assess genomic assignments of individuals. We used R
643 version 3.5.3 (R Core Team 2019) for all analyses.

644

645 **ABBA-BABA tests and admixture graph analysis**

646 We used the four-taxon ABBA-BABA test to understand gene flow among various island
647 populations of babblers (Durand et al. 2011; Green et al. 2010). The ABBA-BABA test is a
648 powerful method to differentiate between secondary admixture and incomplete lineage
649 sorting (Durand et al. 2011; Green et al. 2010). We performed ABBA-BABA tests using
650 ANGSD considering only transversions to account for DNA damage. Only sites with a
651 mapping quality and PHRED score ≥30 were considered. To test for significance, we
652 performed jackknifing of 20kb blocks. Only test scenarios congruent with the phylogenomic
653 analysis were considered. Significant secondary admixture was inferred when Z scores
654 exceeded -3 or +3. For ABBA-BABA analyses, we used the bam files obtained by mapping
655 clean reads to the chromosomal assembly of the great tit genome.

656

657 In addition to ABBA-BABA tests, we performed admixture graph analysis with qpbrute
658 (Leathlobhair et al. 2018; Liu et al. 2019), which implements a heuristic algorithm to
659 iteratively fit complex admixture models using qpGraph (part of ADMIXTOOLS 5.1
660 (Patterson et al. 2012)) as well as estimate Bayes factors to determine the best admixture
661 graph: qpGraph reconstructs relationships among populations using a phylogenetic approach
662 allowing for admixture events. For a given topology, *f2*, *f3* and *f4* statistics are estimated for
663 all taxa and the observed and expected allele frequencies are calculated for the observed data
664 and model. Within qpbrute, for a given outgroup, taxa are added iteratively. If a node cannot
665 initially be included and outliers are observed for the *f4* statistic, then all possible admixture
666 events are attempted. If a node ends up being excluded, its subgraph is discarded, but if a
667 node is successfully included, remaining nodes are added iteratively to the subgraph. All
668 possible combinations of taxa are tested within qpbrute to ensure a complete coverage of
669 graph space. We used dataset IV along with an outgroup and also included SNPs mapping to
670 the Z chromosome for this analysis.

671

672 **REFERENCES**

673 Andrews S. 2010. FastQC: a quality control tool for high throughput sequence data.
674 https://www.bioinformatics.babraham.ac.uk/projects/fastqc/

675

676 Bird MI, Taylor D, Hunt C. 2005. Palaeoenvironments of insular Southeast Asia during the
677 Last Glacial Period: a savanna corridor in Sundaland? *Quat Sci Rev* 24:2228–2242.

678
679 Borregaard MK, Matthews TJ, Whittaker RJ. 2016. The general dynamic model: towards a
680 unified theory of island biogeography? *Glob Ecol Biogeogr* 25:805–816.
681
682 Bolger AM, Lohse M, Usadel B. 2014. Trimmomatic: a flexible trimmer for Illumina
683 sequence data. *Bioinformatics* 30:2114–2120.
684
685 Borowiec ML. 2016. AMAS: a fast tool for alignment manipulation and computing of
686 summary statistics. *PeerJ* 4:e1660.
687
688 Brown RM, Siler CD, Oliveros CH, Esselstyn JA, Diesmos AC, Hosner PA, Linkem CW,
689 Barley AJ, Oaks JR, Sanguila MB, et al. 2013. Evolutionary processes of diversification in a
690 model island archipelago. *Annu Rev Ecol Evol S* 44:411–435.
691
692 Burney CW, Brumfield RT. 2009. Ecology predicts levels of genetic differentiation in
693 Neotropical birds. *Am Nat* 174:358–368.
694
695 Bushnell B. 2014. BBMap: a fast, accurate, splice-aware aligner, Lawrence Berkeley
696 National Lab (LBNL), Berkeley, CA United States.
697
698 Cannon CH, Morley RJ, Bush AB. 2009. The current refugial rainforests of Sundaland are
699 unrepresentative of their biogeographic past and highly vulnerable to disturbance. *Proc Natl*
700 *Acad Sci U.S.A.* 106:11188–11193.
701
702 Castresana J. 2000. Selection of conserved blocks from multiple alignments for their use in
703 phylogenetic analysis. *Mol Biol Evol* 17:540–552.
704
705 Chattopadhyay B, Garg KM, Gwee CY, Edwards SV, Rheindt FE. 2017. Gene flow during
706 glacial habitat shifts facilitates character displacement in a Neotropical flycatcher radiation.
707 *BMC Evol Biol* 17:210.
708
709 Chattopadhyay B, Garg KM, Mendenhall IH, Rheindt FE. 2019. Historic DNA reveals
710 Anthropocene threat to a tropical urban fruit bat. *Curr Biol* 29:R1299–R1300.
711

712 Cros E, Chattopadhyay B, Garg KM, Ng NS, Tomassi S, Benedick S, Edwards DP, Rheindt
713 FE. 2020. Quaternary land bridges have not been universal conduits of gene flow. *Mol Ecol*
714 29:2692–2706.
715
716 Cros E, Ng EY, Oh RR, Tang Q, Benedick S, Edwards DP, Tomassi S, Irestedt M, Ericson
717 PG, Rheindt FE. 2020. Fine-scale barriers to connectivity across a fragmented South-East
718 Asian landscape in six songbird species. *Evol Appl* 13:1026–1036.
719
720 da Costa MJ, do Amaral PJ, Pieczarka JC, Sampaio MI, Rossi RV, Mendes-Oliveira AC,
721 Noronha RC, Nagamachi CY. 2016. Cryptic species in *Proechimys goeldii* (Rodentia,
722 Echimyidae)? A case of molecular and chromosomal differentiation in allopatric populations.
723 *Cytogenet Genome Res* 148:199–210.
724
725 Dabney J, Meyer M, Pääbo S. 2013. Ancient DNA damage. *Cold Spring Harb Perspect Biol*
726 5:a012567.
727
728 Danecek P, Auton A, Abecasis G, Albers CA, Banks E, DePristo MA, Handsaker RE, Lunter
729 G, Marth GT, Sherry ST, et al. 2011.The variant call format and VCFtools. *Bioinformatics*
730 27:2156–2158.
731
732 Durand EY, Patterson N, Reich D, Slatkin M. 2011. Testing for ancient admixture between
733 closely related populations. *Mol Biol Evol* 28:2239–2252.
734
735 Eaton JA, van Balen S, Brickle NW, Rheindt FE. 2016. Birds of the Indonesian Archipelago:
736 Greater Sundas and Wallacea. Lynx Edicions.
737
738 Faircloth BC. 2016. PHYLUCE is a software package for the analysis of conserved genomic
739 loci. *Bioinformatics* 32:786–788.
740
741 Felsenstein J. 2005. PHYLIP version 3.6. Software package distrbuted by the author,
742 Department of Genetics, University of Washington, Seattle.
743

744 Fernández-Palacios JM, Rijsdijk KF, Norder SJ, Otto R, de Nascimento L, Fernández-Lugo
745 S, Tjørve E, Whittaker RJ. 2016. Towards a glacial-sensitive model of island biogeography.
746 *Glob Ecol Biogeogr* 25:817–830.
747
748 Foll M, Gaggiotti O. 2008. A genome-scan method to identify selected loci appropriate for
749 both dominant and codominant markers: a Bayesian perspective. *Genetics* 180:977–993.
750
751 Francis RM. 2017. pophelper: an R package and web app to analyse and visualize population
752 structure. *Mol Ecol Resour* 17:27–32.
753
754 Garg KM, Chattopadhyay B, Wilton PR, Prawiradilaga DM, Rheindt FE. 2018. Pleistocene
755 land bridges act as semipermeable agents of avian gene flow in Wallacea. *Mol Phylogenet*
756 *Evol* 125:196–203.
757
758 Garg KM, Chattopadhyay B, Koane B, Sam K, Rheindt FE. 2020. Last Glacial Maximum
759 led to community-wide population expansion in a montane songbird radiation in highland
760 Papua New Guinea. *BMC Evol Biol* 20:1–10.
761
762 Green RE, Krause J, Briggs AW, Maricic T, Stenzel U, Kircher M, Patterson N, Li H, Zhai
763 W, Fritz MH, et al. 2010. A draft sequence of the Neandertal genome. *Science* 328:710–722.
764
765 Heaney LR. 1986. Biogeography of mammals in SE Asia: estimates of rates of colonization,
766 extinction and speciation. *Biol J Linn Soc* 28:127–165.
767
768 Heaney LR, Walsh Jr JS, Townsend Peterson A. 2005. The roles of geological history and
769 colonization abilities in genetic differentiation between mammalian populations in the
770 Philippine archipelago. *J Biogeogr* 32:229–247.
771
772 Hewitt GM. 2000. The genetic legacy of the Quaternary ice ages. *Nature* 405:907–913.
773
774 Hewitt GM. 2004. Genetic consequences of climatic oscillations in the Quaternary. *Philos*
775 *Trans R Soc B* 359:183–195.
776

Huxley TH. 1868. On the classification and distribution of the Alectoromorphae and Heteromorphae. *Proc Zool Soc Lond* 294–319

Isler ML, Alonso JA, Isler PR, Whitney BM. 2001. A new species of Percnostola antbird (Passeriformes: Thamnophilidae) from Amazonian Peru, and an analysis of species limits within *Percnostola rufifrons*. *Wilson J Ornithol* 113:164–176.

Isler ML, Maldonado-Coelho M. 2017. Calls distinguish species of Antbirds (Aves: Passeriformes: Thamnophilidae) in the genus *Pyriglena*. *Zootaxa* 4291:275–294.

Johnson MG, Gardner EM, Liu Y, Medina R, Goffinet B, Shaw AJ, Zerega NJ, Wickett NJ. 2016. HybPiper: Extracting coding sequence and introns for phylogenetics from high-throughput sequencing reads using target enrichment. *Appl Plant Sci* 4:1600016.

Jombart T. 2008. adegenet: a R package for the multivariate analysis of genetic markers. *Bioinformatics* 24:1403–1405.

Jónsson H, Ginolhac A, Schubert M, Johnson PL, Orlando L. 2013. mapDamage2.0: fast approximate Bayesian estimates of ancient DNA damage parameters. *Bioinformatics* 29:1682–1684.

Kircher M, Sawyer S, Meyer M. 2012. Double indexing overcomes inaccuracies in multiplex sequencing on the Illumina platform. *Nucleic Acids Res* 40:e3.

Leathlobhair MN, Perri AR, Irving-Pease EK, Witt KE, Linderholm A, Haile J, Lebrasseur O, Ameen C, Blick J, Boyko AR. 2018. The evolutionary history of dogs in the Americas. *Science* 361:81–85.

Leonard JA, den Tex RJ, Hawkins MT, Muñoz-Fuentes V, Thorington R, Maldonado JE. 2015. Phylogeography of vertebrates on the Sunda Shelf: a multi-species comparison. *J Biogeogr* 42:871–879.

809 Li C, Riethoven JJM, Naylor GJ. 2012. EvolMarkers: a database for mining exon and intron
810 markers for evolution, ecology and conservation studies. *Mol Ecol Resour* 12:967–971.
811
812 Li H, Durbin R. 2009. Fast and accurate short read alignment with Burrows–Wheeler
813 transform. *Bioinformatics* 25:1754–1760.
814
815 Li H, Handsaker B, Wysoker A, Fennell T, Ruan J, Homer N, Marth G, Abecasis G, Durbin
816 R. 2009. The sequence alignment/map format and SAMtools. *Bioinformatics* 25:2078–2079.
817
818 Li, H. 2011. A statistical framework for SNP calling, mutation discovery, association
819 mapping and population genetical parameter estimation from sequencing data. *Bioinformatics*
820 27:2987–2993.
821
822 Lim HC, Sheldon FH. 2011. Multilocus analysis of the evolutionary dynamics of rainforest
823 bird populations in Southeast Asia. *Mol Ecol* 20:3414–3438 (2011).
824
825 Lim HC, Rahman MA, Lim SL, Moyle RG, Sheldon FH. 2011. Revisiting Wallace's haunt:
826 Coalescent simulations and comparative niche modeling reveal historical mechanisms that
827 promoted avian population divergence in the Malay Archipelago. *Evolution* 65:321–334.
828
829 Lim HC, Gawin DF, Shakya SB, Harvey MG, Rahman MA, Sheldon FH. 2017. Sundaland's
830 east–west rain forest population structure: variable manifestations in four polytypic bird
831 species examined using RAD-Seq and plumage analyses. *J Biogeogr* 44:2259–2271.
832
833 Liu L, Yu L, Edwards SV. 2010. A maximum pseudo-likelihood approach for estimating
834 species trees under the coalescent model. *BMC Evol Biol* 10:302.
835
836 Liu L, Zhang J, Rheindt FE, Lei F, Qu Y, Wang Y, Zhang Y, Sullivan C, Nie W, Wang J, et
837 al. 2017. Genomic evidence reveals a radiation of placental mammals uninterrupted by the
838 KPg boundary. *Proc Natl Acad Sci U.S.A.* 114:E7282–E7290.
839
840 Liu L, Bosse M, Megens HJ, Frantz LA, Lee YL, Irving-Pease EK, Narayan G, Groenen MA,
841 Madsen O. 2019. Genomic analysis on pygmy hog reveals extensive interbreeding during
842 wild boar expansion. *Nat Commun* 10:1–9.

Liu L, Bosse M, Megens HJ, Frantz LA, Lee YL, Irving-Pease EK, Narayan G, Groenen MA, Madsen O. Genomic analysis on pygmy hog reveals extensive interbreeding during wild boar expansion. Nature communications. 2019 Apr 30;10(1):1-9.

Lohman DJ, de Bruyn M, Page T, von Rintelen K, Hall R, Ng PK, Shih HT, Carvalho GR, Von Rintelen T. 2011. Biogeography of the Indo-Australian archipelago. *Annu Rev Ecol Evol S* 42:205–226.

Katoh K, Standley DM. 2016. A simple method to control over-alignment in the MAFFT multiple sequence alignment program. *Bioinformatics* 32:1933–1942.

Korneliussen TS, Albrechtsen A, Nielsen R. 2014. ANGSD: analysis of next generation sequencing data. *BMC Bioinformatics* 15:356.

MacArthur RH, Wilson EO. 1967. The Theory of Island Biogeography. New Jersey: Princeton University Press.

Martin M. 2011. Cutadapt removes adapter sequences from high-throughput sequencing reads. *EMBnet Journal* 17:10–12.

Mason VC, Helgen KM, Murphy WJ. 2019. Comparative phylogeography of forest-dependent mammals reveals Paleo-forest corridors throughout Sundaland. *J Hered* 110:158–172.

Mayr E, Diamond JM, Diamond J. 2001. The Birds of Northern Melanesia: Speciation, Ecology & Biogeography. Oxford: Oxford University Press.

Mays Jr HL, Hung CM, Shaner PJ, Denvir J, Justice M, Yang SF, Roth TL, Oehler DA, Fan J, Rekulapally S, et al. 2018. Genomic analysis of demographic history and ecological niche modeling in the endangered Sumatran rhinoceros Dicerorhinus sumatrensis. *Curr Biol* 28: 70–76.

876 Moyle RG, Filardi CE, Smith CE, Diamond J. 2009. Explosive Pleistocene diversification
877 and hemispheric expansion of a "great speciator". *Proc Natl Acad Sci U.S.A.* 106:1863–1868.
878
879 Nater A, Mattle-Greminger MP, Nurcahyo A, Nowak MG, De Manuel M, Desai T, Groves
880 C, Pybus M, Sonay TB, Roos C, Lameira AR. 2017. Morphometric, behavioral, and genomic
881 evidence for a new orangutan species. *Curr Biol* 27:3487–3498. e3410.
882
883 Ng NS, Wilton PR, Prawiradilaga DM, Tay YC, Indrawan M, Garg KM, Rheindt FE. 2017.
884 The effects of Pleistocene climate change on biotic differentiation in a montane songbird
885 clade from Wallacea. *Mol Phylogenet Evol* 114:353–366.
886
887 Papadopoulou A, Knowles LL. 2017. Linking micro-and macroevolutionary perspectives to
888 evaluate the role of Quaternary sea-level oscillations in island diversification. *Evolution*
889 71:2901–2917.
890
891 Patterson N, Moorjani P, Luo Y, Mallick S, Rohland N, Zhan Y, Genschoreck T, Webster T,
892 Reich D. 2012. Ancient admixture in human history. *Genetics* 192:1065–1093.
893
894 Pritchard JK, Stephens M, Donnelly P. 2000. Inference of population structure using
895 multilocus genotype data. *Genetics* 155:945–959.
896
897 Prüfer K, Munch K, Hellmann I, Akagi K, Miller JR, Walenz B, Koren S, Sutton G, Kodira
898 C, Winer R, et al. 2012. The bonobo genome compared with the chimpanzee and human
899 genomes. *Nature* 486:527–531.
900
901 Purcell S, Neale B, Todd-Brown K, Thomas L, Ferreira MA, Bender D, Maller J, Sklar P, De
902 Bakker PI, Daly MJ, et al. 2007. PLINK: a tool set for whole-genome association and
903 population-based linkage analyses. *Am J Hum Genet* 81:559–575.
904
905 Quinlan AR, Hall IM. 2010. BEDTools: a flexible suite of utilities for comparing genomic
906 features. *Bioinformatics* 26:841–842.
907
908 R Core Team. 2019. R: A language and environment for statistical computing.
909

910 Rheindt FE, Christidis L, Norman JA. 2008. Habitat shifts in the evolutionary history of a
911 Neotropical flycatcher lineage from forest and open landscapes. *BMC Evol Biol* 8:193.
912
913 Rheindt FE, Christidis L, Cabanne GS, Miyaki C, Norman JA. 2009. The timing of
914 neotropical speciation dynamics: a reconstruction of *Myiopagis* flycatcher diversification
915 using phylogenetic and paleogeographic data. *Mol Phylogenet Evol* 53:961–971.
916
917 Rheindt FE, Prawiradilaga DM, Ashari H, Gwee CY, Lee GW, Wu MY, Ng NS. 2020. A lost
918 world in Wallacea: Description of a montane archipelagic avifauna. *Science* 367:167–170.
919
920 Robson C. 2005. Birds of Southeast Asia. New Jersey: Princeton Univrsity Press.
921
922 Sadanandan KR, Rheindt FE. 2015. Genetic diversity of a tropical rainforest understory bird
923 in an urban fragmented landscape. *Condor* 117:447–459.
924
925 Sathiamurthy E, Voris HK. 2006. Maps of Holocene sea level transgression and submerged
926 lakes on the Sunda Shelf. *Trop Nat Hist* 1–44.
927
928 Sarr AC, Husson L, Sepulchre P, Pastier AM, Pedoja K, Elliot M, Arias-Ruiz C, Solihuddin
929 T, Aribowo S. 2019. Subsiding Sundaland. *Geology* 47:119–122.
930
931 Smit A, Hubley R, Green P. 2015. RepeatMasker Open-4.0. [Internet]. 2013–2015. Available
932 from: http://www.repeatmasker.org/.
933
934 Stamatakis A. 2014. RAxML version 8: a tool for phylogenetic analysis and post-analysis of
935 large phylogenies. *Bioinformatics* 30:1312–1313.
936
937 Sterrer W, Glasspool A, De Silva H, Furbert J. 2004. Bermuda—an island biodiversity
938 transported. In: Davenport J, Davenport J, editors. The effects of human transport on
939 ecosystems: cars and planes, boats and trains. Dublin: Royal Irish Academy. P. 118–170.
940
941 Taberlet P, Fumagalli L, Wust-Saucy AG, Cosson JF. 1998. Comparative phylogeography
942 and postglacial colonization routes in Europe. *Mol Ecol* 7:453–464.
943

944 Teacher A, Garner T, Nichols R. 2009. European phylogeography of the common frog (*Rana*
945 *temporaria*): routes of postglacial colonization into the British Isles, and evidence for an Irish
946 glacial refugium. *Heredity* 102:490–496.
947
948 Voris HK. 2000. Maps of Pleistocene sea levels in Southeast Asia: shorelines, river systems
949 and time durations. *J Biogeogr* 27:1153–1167.
950
951 Wallace AR. 1860. On the zoological geography of the Malay Archipelago. *J Proc Linn Soc*
952 4:172–184.
953
954 Wallace A. 1872. Flora and Fauna of the Azores. *Am Nat* 6:176–177.
955
956 Weigelt P, Steinbauer MJ, Cabral JS, Kreft H. 2016. Late Quaternary climate change shapes
957 island biodiversity. *Nature* 532:99–102.
958
959 Whittaker RJ, Fernández-Palacios JM, Matthews TJ, Borregaard MK, Triantis KA. 2017.
960 Island biogeography: Taking the long view of nature's laboratories. *Science* 357:885–892.
961
962 Zakaria M, Rajpar MN, Moradi HV, Rosli Z. 2013. Comparison of understorey bird species
963 in relation to edge–interior gradient in an isolated tropical rainforest of Malaysia. *Environ*
964 *Dev Sustain* 16:375–392.
965
966 Zheng X, Levine D, Shen J, Gogarten SM, Laurie C, Weir BS. 2012. High-performance
967 computing toolset for relatedness and principal component analysis of SNP data.
968 *Bioinformatics* 28:3326–3328.
969

970 **ACKNOWLEDGMENTS**

971 This study was supported by a South East Asian Biodiversity Genomics (SEABIG) grant
972 (WBS R-154-000-648-646 and WBS R-154-000-648-733) and a Singapore Ministry of
973 Education Tier II grant (WBS R-154-000-A59–112 to F.E.R.). B.C. acknowledges the startup
974 funding from Trivedi School of Biosciences, Ashoka University, India and K.M.G.
975 acknowledges the support from the DBT-Ramalingaswami Fellowship (No.
976 BT/HRD/35/02/2006). The authors thank Kelvin Lim at the Lee Kong Chian Natural History
977 Museum and Kristof Zyskowski at the Yale Peabody Museum of Natural History for

providing toepad samples and Dr. Lau On Sun for help with the bioruptor. The authors thank Chyi Yin Gwee, Pratibha Baveja, Tang Qian, Arina Adom, Ling Lih Chua and Lu Wee Tan for logistical and lab assistance and Evan K. Irving-Pease for help with qpBrute.

ETHICS STATEMENT

This study complied with all ethical regulations. Protocols were approved by the National University of Singapore Institutional Animal Care and Use Committee (IACUC, Protocol Number: L2017–00459). Permits for sampling in Sabah were approved by the Danum Valley Management Committee, the Sabah Forestry Department, and the Sabah Biodiversity Council (permit numbers: JKM/MBS.1000-2/2 JLD.3 (118); JHL 100.7/27 and export samples [permit number: JKM/MBS.1000-2/3 JLD.2 (65)).

AUTHOR CONTRIBUTIONS

KMG and FER designed the research. KMG performed laboratory work with input from BC. KMG and BC designed the target enrichment loci with input from FER. EC performed toepad sampling and plumage analysis. EC conducted fieldwork with the help of SB, ST and DPE. KMG and FER wrote the paper with input from all co-authors.

COMPETING INTERESTS

The authors declare no competing interests.

DATA AVAILABILITY

The data underlying this article are available in the article and in its online supplementary material. Raw data generated in this study have been submitted to the NCBI SRA database (BioProject ID: PRJNA701111).

1012 **FIGURES**

1013

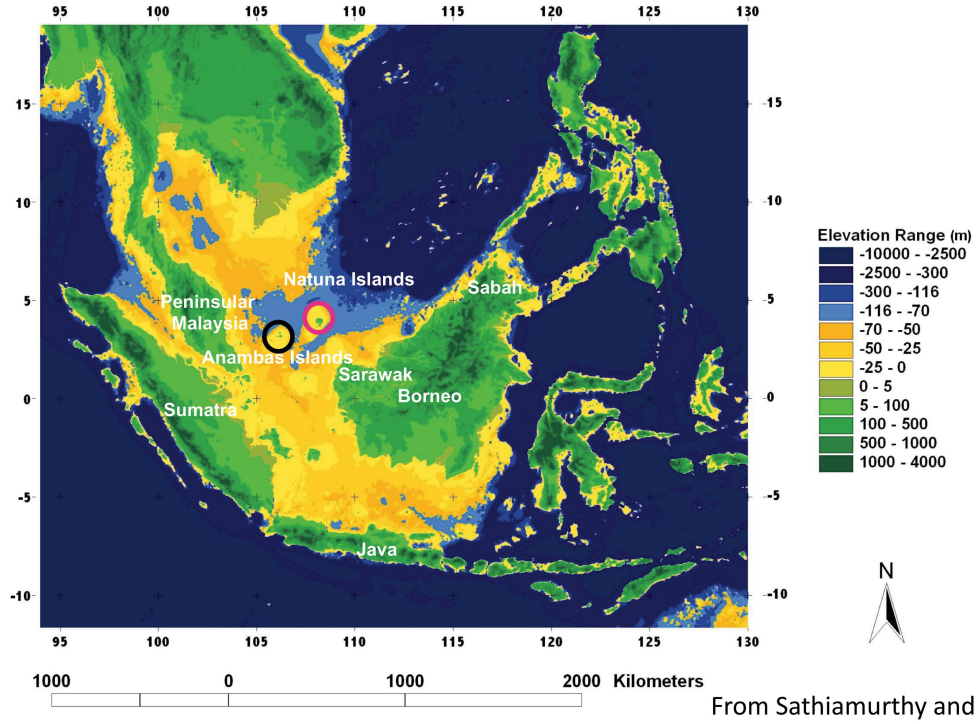

From Sathiamurthy and Voris (2006)
Modified with permission

1014

1015 Fig. 1: Map showing Sundaland and sea depths across the Sunda Shelf. Note that land would
1016 have extended approximately to the -116m isobath (border between light-blue and mid-blue)
1017 at the peak of glacial episodes.

1018

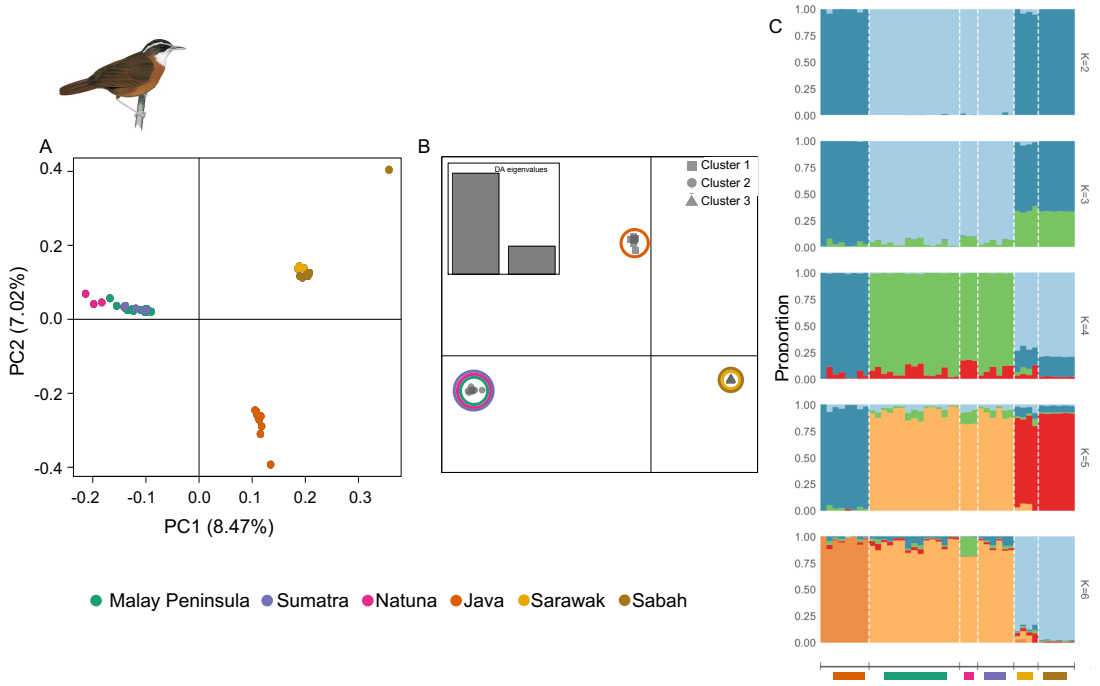

1019

1020 Fig. 2: Population subdivision observed in *Pellorneum capistratum* based on transversions
1021 isolated after mapping to the *Parus major* genome. Three population clusters observed based
1022 on (A) principal component (PC) analysis (number of transversions = 10,848), (B)
1023 discriminant analysis (DA) of principal components, in which clusters are color coded based
1024 on population affinity (number of transversions = 38,463), (C) genetic assignment of *P.*
1025 *capistratum* individuals using STRUCTURE for K=2 to K=6 (number of transversions =
1026 38,463).

1027

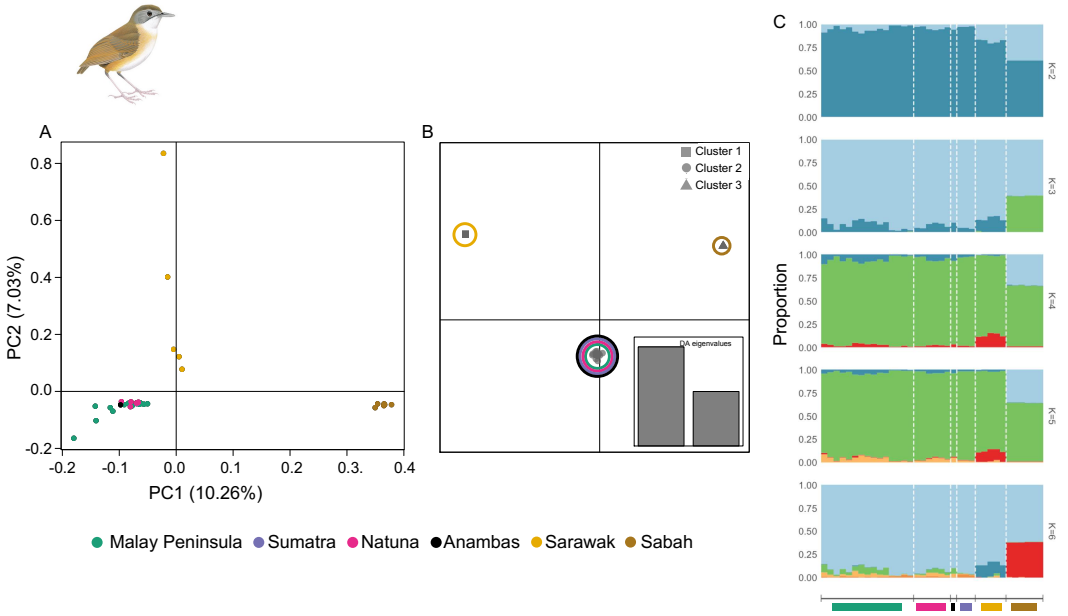

Fig. 3: Population subdivision observed in *Pellorneum malaccense* based on transversions isolated after mapping to the *Parus major* genome. Three population clusters observed based on (A) principal component (PC) analysis (number of transversions = 6,091), (B) discriminant analysis (DA) of principal components, in which clusters are color coded based on population affinity (number of transversions = 32,735), (C) genetic assignment of *P. malaccense* individuals using STRUCTURE for K=2 to K=6 (number of transversions = 32,735).

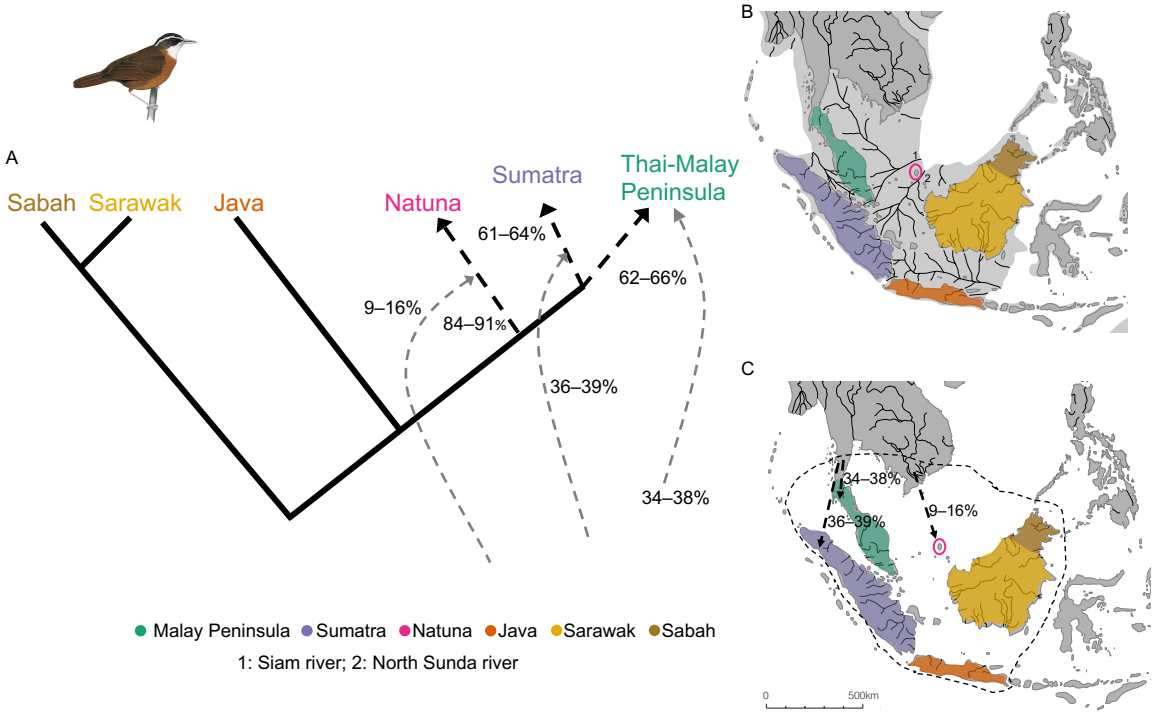

1037

1038 Fig. 4: Admixture graph of gene flow dynamics observed in *Pellorneum capistratum*. (A)
1039 Schematic of genetic ancestry and admixture proportions among populations of *P.*
1040 *capistratum* based on a combination of five best-fit admixture graphs, all of which exhibited
1041 an identical topology and only differed slightly in estimates of the extent of admixture from
1042 an unknown source for the western Sundaic population; (B) map during sea level recession of
1043 ~120m at glacial maximum around 20,000 years before present, showing major paleo-rivers
1044 and present-day taxon distributions; (C) current map of South East Asia with taxon
1045 distributions, major rivers, and arrows indicating potential gene flow from unsampled or
1046 extinct populations (see panel A). The black stippled line indicates potential habitat during
1047 sea level lows. Panels B and C modified with permission from Voris (2000).

1048

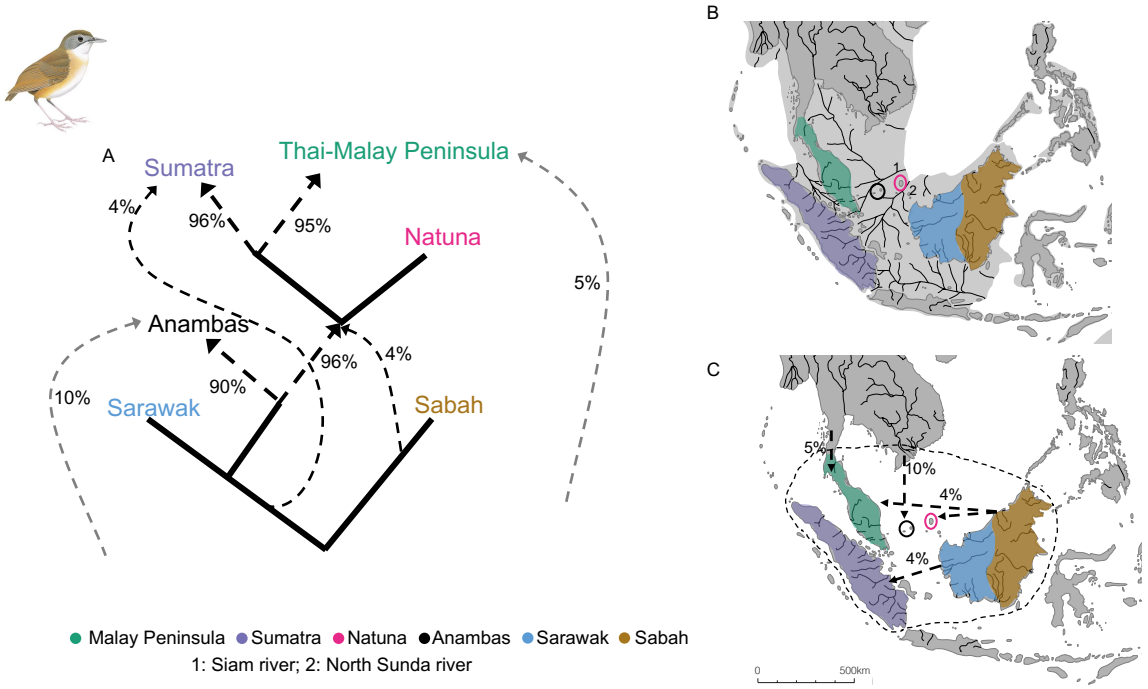

1049

1050 Fig. 5: Admixture graph of gene flow dynamics observed in *Pellorneum malaccense.* (A)
1051 Schematic of genetic ancestry and admixture proportions among populations of *P.*
1052 *malaccense* based on single best-fit admixture graph; (B) map during sea level recession of
1053 ~120m at glacial maximum around 20,000 years before present, showing major paleo-rivers
1054 and present-day taxon distributions; (C) current map of South East Asia with taxon
1055 distributions, major rivers, and arrows indicating potential gene flow among populations or
1056 from unsampled or extinct populations (see panel A). The black stippled line indicates
1057 potential habitat during sea level lows. Panels B and C modified with permission from Voris
1058 (2000).

1059 **TABLES**

1060

1061 Table 1: Number of SNPs identified and filtered for different datasets. Abbreviations: HWE – Hardy-Weinberg equilibrium; NA – not
1062 applicable.

1063

Dataset	Number of unfiltered SNPs	Number of SNPs removed due to linkage	Number of SNPs removed that were not in HWE	Number of non-neutral SNPs removed	Number of SNPs removed mapping to Z chromosome	Number of transitions removed	Number of SNPs retained	Number of SNPs with no missing data
Pellorneum capistratum								
Dataset I: All SNPs obtained after mapping to *Mixornis gularis* genome	82,468	24,025	1,904	82	1,246	NA	54,906	54,906
Dataset II: Only transversions obtained after mapping to	82,468	24,025	1,904	82	1,246	37,690	17,216	17,216

Mixornis gularis genome								
Dataset III: single random SNP per target locus	960	NA	30	12	35	NA	883	883
Dataset IV: Only transversions obtained after mapping to *Parus major* genome	208,186	67,451	3,357	1,130	1,470	96,315	38,463	10,848
Pellorneum malaccense								
Dataset I: All SNPs obtained after mapping to *Mixornis gularis* genome	57,300	21,595	440	240	1,317	NA	33,708	33,708
Dataset II: Only transversions obtained after mapping to	57,300	21,595	440	240	1,317	22,558	11,150	11,150

Mixornis gularis genome								
Dataset III: single random SNP per target locus	958	NA	17	2	44	NA	895	895
Dataset IV: Only transversions obtained after mapping to *Parus major* genome	198,711	83,460	749	1,490	1,491	78,786	32,735	6,091

1064